



# Structural, spectral, thermal and biological studies on 2-oxo-N'-((4-oxo-4H-chromen-3-yl)methylene)-2-(phenylamino)acetohydrazide (H<sub>2</sub>L) and its metal complexes

Ola A. El-Gammal, Gaber Abu El-Reash\*, Sara F. Ahmed

Department of Chemistry, Faculty of Science, Mansoura University, Mansoura, P.O.Box 70, Mansoura, Egypt

## ARTICLE INFO

### Article history:

Received 30 November 2010

Received in revised form 15 March 2011

Accepted 18 March 2011

Available online 25 March 2011

### Keywords:

2-Oxo-N'-((4-oxo-4H-chromen-3-yl)methylene)-2-(phenylamino)acetohydrazide (H<sub>2</sub>L)  
Coats–Redfern  
Horowitz–Metzger  
Antimicrobial activity  
Hydrazone derivatives

## ABSTRACT

A new series of metal complexes formed by the reaction of 2-oxo-N'-((4-oxo-4H-chromen-3-yl)methylene)-2-(phenylamino)acetohydrazide(H<sub>2</sub>L) and Cu(II), Co(II), Ni(II), Cd(II), Zn(II), Hg(II) and U(VI)O<sub>2</sub><sup>2+</sup> ions. The isolated complexes have been characterized by elemental analyses, spectral (IR, UV–visible and <sup>1</sup>H NMR) as well as magnetic and thermal measurements. The data revealed that the ligand acts as neutral ON or ONO as well as mononegative ONO. On the basis of magnetic and electronic spectral data an octahedral geometry for the Co(II), Cu(II) and U(VI)O<sub>2</sub> complexes, a tetrahedral structure for the Ni(II), Cd(II), Zn(II) and Hg(II) complexes have been proposed. The bond length, bond angle, HOMO, LUMO, dipole moment and charges on the atoms have been calculated to confirm the geometry of the ligand and the investigated complexes. Also, kinetic parameters were determined for each thermal degradation stage of some complexes using Coats–Redfern and Horowitz–Metzger methods. Moreover, the ligand and its complexes were screened against *Bacillus thuringiensis* (*Bt*) as Gram positive bacteria and *Pseudomonas aeruginosa* (*Pa*) Gram negative bacteria using the inhibitory zone diameter.

© 2011 Elsevier B.V. All rights reserved.

## 1. Introduction

Hydrazones are important class of ligands which present in numerous physiological and biological applications as antimicrobial, antitumour agents, insecticides, anticoagulants, anticonvulsant, analgesic, antioxidants, anti-inflammatory, antiplatelet, antitubercular and plant growth regulators [1–4].

Metal complexes of hydrazones have found applications as catalysts [5], luminescent probes [6], nonlinear optics and molecular sensors [7]. Moreover, it has been recently shown that pyridoxal isonicotinyl hydrazone can be used in the treatment of iron overload [8].

Chromone derivatives offered interesting possibilities from the point of view of both organic synthesis and assays of their biological activity [9]. We were thus motivated to undertake a systematic study of preparation and characterization of a new transition metal complexes formed with 2-oxo-N'-((4-oxo-4H-chromen-3-yl)methylene)-2-(phenylamino)acetohydrazide (H<sub>2</sub>L) and Cu(II), Co(II), Ni(II), Cd(II), Zn(II), Hg(II) and U(VI)O<sub>2</sub><sup>2+</sup> ions. Also, the thermal degradation and kinetic parameters such as energy of activation (*E<sub>a</sub>*) and the pre-exponential factor (*A*); and thermodynamic param-

eters as entropy ( $\Delta S$ ), enthalpy ( $\Delta H$ ) and free energy ( $\Delta G$ ) for each step of degradation have been evaluated. In addition the antibacterial activity of the ligand and its metal complexes against (*Bt*) as Gram positive bacteria and (*Pa*) as Gram negative bacteria using the inhibitory zone diameter was evaluated.

## 2. Experimental

### 2.1. Instrumentation and materials

All the chemicals were purchased from Aldrich and Fluka and used without further purification. Elemental analyses (C, H and N) were performed with a Perkin–Elmer 2400 series II analyzer. IR spectra (4000–400 cm<sup>-1</sup>) for KBr discs were recorded on a Mattson 5000 FTIR spectrophotometer. Electronic spectra were recorded on a Unicam UV–Vis spectrophotometer UV2. Magnetic susceptibilities were measured with a Sherwood scientific magnetic susceptibility balance at 298 K. <sup>1</sup>H NMR measurements in d<sub>6</sub>-DMSO at room temperature were carried out on a Varian Gemini WM-200 MHz spectrometer at the Microanalytical Unit, Cairo University. Thermogravimetric measurements (TGA, DTA, 20–1000 °C) were recorded on a DTG-50 Shimadzu thermogravimetric analyzer at a heating rate of 10 °C/min and nitrogen flow rate of 20 ml/min.

\* Corresponding author.

E-mail address: [gaelreash@mans.edu.eg](mailto:gaelreash@mans.edu.eg) (G.A. El-Reash).

## 2.2. Synthesis of H<sub>2</sub>OCAH

2-hydrazino-2-oxo-N-phenyl-acetamide 2-Hydrazino-2-oxo-N-phenyl-acetamide was synthesized according to the general literature method [10]. H<sub>2</sub>L was synthesized by heating under reflux for 4 h an ethanolic solution of 2-hydrazino-2-oxo-N-phenyl-acetamide in a 1:1 molar ratio with 3-chromonaldehyde. The pale yellow precipitate was filtered off, washed several times with ethanol and recrystallized from hot ethanol and finally dried in vacuum desiccator over anhydrous CaCl<sub>2</sub>.

## 2.3. Synthesis of metal complexes

A hot ethanolic solution of the respective metal chlorides Co(II), Ni(II), Cu(II), Cd(II), Hg(II) or acetates (Zn(II) and U(VI)O<sub>2</sub>) (1.0 mmol) was added to hot ethanolic solution of H<sub>2</sub>L (0.335 g, 1.0 mmol). The resultant mixture was heated under reflux for 2–3 h, 0.5 gm of sodium acetate in 30 ml bidistilled water was added as a buffering agent except in case of zinc and uranyl complexes. The formed precipitates were filtered off, washed with ethanol followed by diethyl ether and dried in a vacuum desiccator over anhydrous CaCl<sub>2</sub>. The physical and analytical data of the isolated complexes are listed in Table 1. The complexes have high melting points and insoluble in common organic solvents; partially soluble in DMSO and DMF and found to be non-electrolytes.

## 2.4. Antibacterial activity

The *in vitro* antibacterial of the reported complexes was evaluated against *Bacillus thuringiensis* (Bt) as Gram positive and *Pseudomonas aeruginosa* (Pa) Gram negative bacterial cultures using Gentamicin as standard control. The hole plate diffusion method [11] was adopted for the activity measurements. The bacterial strains were grown in nutrient agar slants. A suspension of the studied compounds (0.2 ml of each (10 µg/ml) was incubated at 36 °C for 36 h for the bacterial culture. After inoculation, the diameter (in mm) of the clear inhibition zone surrounding the sample is taken as a measure of the inhibition power against the particular organisms. The experiments were repeated three times and the values recorded are the mean average.

## 2.5. Molecular modeling

An attempt to gain a better insight on the molecular structure of the ligand and its complexes, geometry optimization and conformational analysis has been performed by the use of MM + force-field as implemented in hyperchem 8.0 [12]. The low lying obtained from MM + was then optimized at PM3 using the Polak–Ribiere algorithm in RHF–SCF, set to terminate at an RMS gradient of 0.01 kcal mol<sup>-1</sup>.

## 3. Results and discussion

### 3.1. IR and <sup>1</sup>H NMR spectra

The most important IR bands of H<sub>2</sub>L (Structure 1) and its complexes with probable assignments are given in Table 2. The ligand has multi-coordination sites which gave variable coordination modes. A comparison of the spectrum of H<sub>2</sub>L and those of complexes revealed that the ligand coordinates in the keto and enol forms. H<sub>2</sub>L shows two bands at 1566 and 1598 cm<sup>-1</sup> assignable to ν(C=N) (azomethine) and ν(C=C)phenyl vibrations, respectively [13]. The two sharp bands located at 1680 and 1639 cm<sup>-1</sup> are attributed to ν(C=O) (Chromonic) and [ν(C=O)<sup>2</sup> + ν(C=O)<sup>3</sup>]- (hydrazonic) vibrations, respectively. The medium bands observed at 3284 and 3252 cm<sup>-1</sup> are attributable to ν(N<sup>1</sup>H) [14] and ν(N<sup>4</sup>H) [15] vibrations, respectively. The medium intensity band at 1084 cm<sup>-1</sup> is referred to ν(N–N) vibration [16]. The absence of hydrogen bond does not suggest the hydrogen bonding [17].

The <sup>1</sup>H NMR spectrum of H<sub>2</sub>L in d<sub>6</sub>-DMSO shows two signals at δ=10.06 and 10.27 ppm relative to TMS assignable to N<sup>1</sup>H and N<sup>4</sup>H [14] protons, respectively. The multiplets at 7.00–8.50 ppm are assigned to the phenyl ring protons [18], while the signals at 8.6 and 8.7 ppm are due to CH<sub>(chromonic)</sub> proton [19] and CH proton [20] of azomethine group, respectively.

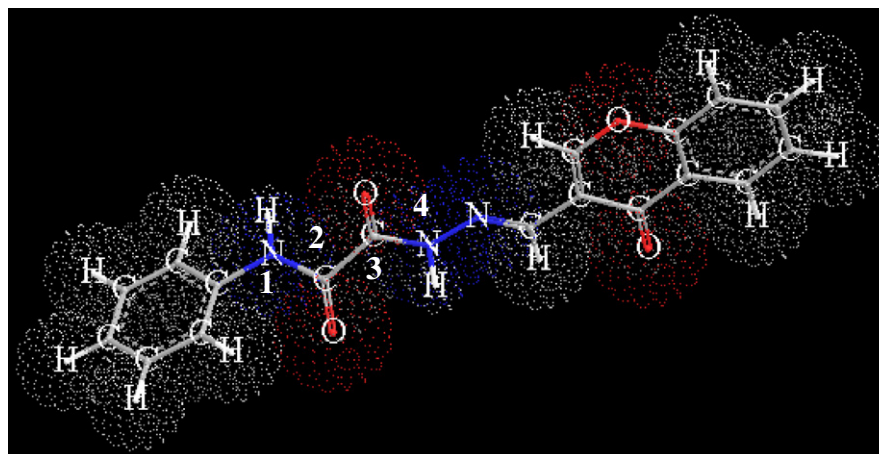
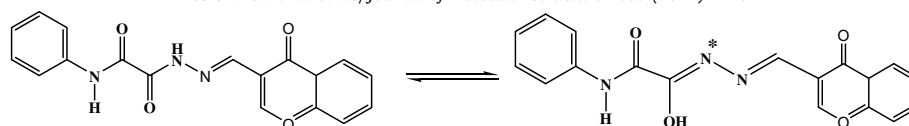
The position of the bands assigned to ν(C=O)<sup>2</sup>(hydrazonic) and ν(N<sup>1</sup>H) vibrations remaining unchanged in all complexes indicating that these groups are not involved in coordination.

IR spectrum of [Co(H<sub>2</sub>L)Cl<sub>2</sub>(H<sub>2</sub>O)<sub>2</sub>] complex indicates that H<sub>2</sub>L behaves as a neutral NO bidentate via C=N(azomethine) and C=O(chromonic) groups (Structure 2). This behavior is revealed by the shift of ν(C=N) and ν(C=O)(chromonic) bands to lower wavenumber. The ν(N–N) vibration shifts to lower wavenumber confirming contribution of azomethine group in coordination [17] and ν(C=O)<sup>3</sup>(hydrazonic) band remains practically unaltered indicating that this group is not participated in bonding.

In [Hg(H<sub>2</sub>L)Cl<sub>2</sub>](H<sub>2</sub>O) (Structure 3) and [UO<sub>2</sub>(H<sub>2</sub>L)(OAc)<sub>2</sub>](H<sub>2</sub>O) complexes, H<sub>2</sub>L coordinates as a neutral NO bidentate through C=N(azomethine) and C=O<sup>3</sup> (hydrazonic) groups. This mode of chelation is confirmed by the shift of ν(C=N)(azomethine) and ν(C=O)<sup>3</sup>(hydrazonic) to lower wavenumber. The presence of ν(C=O)(chromonic) band at the same position suggesting that this group is not participating in coordination. The broad bands observed at 1553 and 1431 cm<sup>-1</sup> assignable to ν<sub>as</sub>(OCO) and ν<sub>s</sub>(OCO) vibrations, respectively with frequency difference (Δν = 122 cm<sup>-1</sup>) [21] confirming monodentate nature of the acetate group [22]. Moreover, the IR spectrum exhibits two bands at 914 and 820 cm<sup>-1</sup>, assignable to asymmetric stretching frequency (ν<sub>3</sub>) and symmetric stretching frequency (ν<sub>1</sub>), respectively, of the dioxouranium ion [17,23]. The force constant (F) for the bonding sites of ν(U=O) is calculated by the method of McGlynn et al. [24]; F<sub>U–O</sub> value is found to be 6.89 mdynes Å<sup>-1</sup>. Also, the U–O bond distance is calculated by the method of Jones; [25] R<sub>U–O</sub> value is 1.73 Å fall-

**Table 1**  
Analytical and physical data of H<sub>2</sub>L and its metal complexes.

Compound, empirical formula, (F:Wt)	Color	M.p. (°C)	% Found (Calcd.)				Yield (%)
			M	Cl	C	H	
H <sub>2</sub> L, C <sub>18</sub> H <sub>13</sub> N <sub>3</sub> O <sub>4</sub> , (335.3)	Pale yellow	270	–	–	63.10 (64.47)	3.19 (3.91)	93
[Cu(H <sub>2</sub> L)Cl <sub>2</sub> (H <sub>2</sub> O)]H <sub>2</sub> O, C <sub>18</sub> H <sub>17</sub> Cl <sub>2</sub> CuN <sub>3</sub> O <sub>6</sub> , (505.8)	Green	>300	12.10 (12.56)	14.31 (14.02)	42.86 (42.74)	3.22 (3.39)	80
[Co(H <sub>2</sub> L)Cl <sub>2</sub> (H <sub>2</sub> O) <sub>2</sub> ], C <sub>18</sub> H <sub>17</sub> Cl <sub>2</sub> CoN <sub>3</sub> O <sub>6</sub> , (501.2)	Reddish brown	>300	11.90 (11.76)	13.89 (14.15)	43.09 (43.14)	2.88 (3.42)	84
[Ni(HL)Cl], C <sub>18</sub> H <sub>12</sub> ClN <sub>3</sub> NiO <sub>4</sub> , (428.5)	Green	>300	13.15 (13.69)	8.33 (8.27)	50.33 (50.45)	2.99 (2.82)	86
[Cd(HL)Cl]H <sub>2</sub> O, C <sub>18</sub> H <sub>14</sub> CdClN <sub>3</sub> O <sub>5</sub> , (500.2)	Pale yellow	294	21.98 (22.47)	6.88 (7.09)	43.10 (43.22)	2.75 (2.82)	72
[Zn(HL)(OAc)]H <sub>2</sub> O, C <sub>20</sub> H <sub>17</sub> N <sub>3</sub> O <sub>7</sub> Zn, (476.8)	Orange	>300	13.20 (13.72)	–	50.24 (50.39)	3.11 (3.59)	81
[Hg(H <sub>2</sub> L)Cl <sub>2</sub> ](H <sub>2</sub> O), C <sub>18</sub> H <sub>15</sub> Cl <sub>2</sub> HgN <sub>3</sub> O <sub>5</sub> , (624.8)	Pale yellow	295	32.80 (32.10)	10.91 (11.35)	33.87 (34.60)	2.01 (2.42)	76
[UO <sub>2</sub> (H <sub>2</sub> L)(OAc) <sub>2</sub> ](H <sub>2</sub> O), C <sub>22</sub> H <sub>21</sub> N <sub>3</sub> O <sub>11</sub> U, (741.4)	Deep brown	>300	32.01 (32.10)	–	35.33 (35.64)	2.56 (2.85)	78

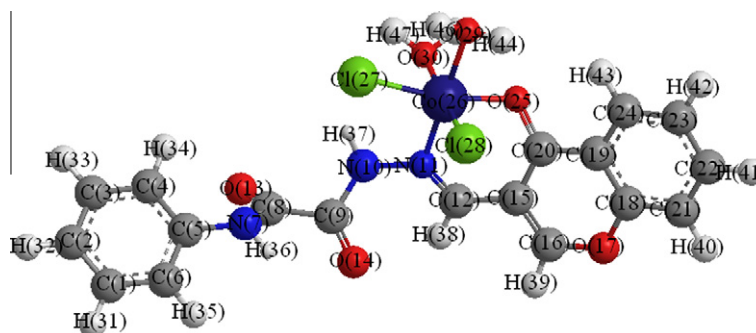
Structure 1. H<sub>2</sub>L.

**Table 2**  
Principle infrared bands of H<sub>2</sub>L and its metal complexes.

Compound	$\nu(\text{C}=\text{N})$	$\nu(\text{C}=\text{O})^2$	$\nu(\text{C}=\text{O})^3$	$\nu(\text{C}=\text{O})_{\text{Chr}}$	$\nu(\text{N}^4\text{H})$	$\nu(\text{C}-\text{O})$	$\nu(\text{N}-\text{N})$	$\nu(\text{C}=\text{N})^*$	$\nu(\text{M}-\text{O})$	$\nu(\text{M}-\text{N})$
H <sub>2</sub> L	1566	1639	1639	1680	3252	–	1084	–	–	–
[Cu(H <sub>2</sub> L)Cl <sub>2</sub> (H <sub>2</sub> O)]H <sub>2</sub> O	1521	1641	1617	1677	3252	–	1060	–	501	434
[Co(H <sub>2</sub> L)Cl <sub>2</sub> (H <sub>2</sub> O) <sub>2</sub> ]	1550	1639	1639	1665	3253	–	1060	–	500	473
[Ni(HL)Cl]	1554	1642	–	1658	–	1108	1074	1610	500	474
[Cd(HL)Cl]H <sub>2</sub> O	1573	1643	–	1666	–	1114	1074	1616	514	460
[Zn(HL)(OAc)]H <sub>2</sub> O	1575	1644	–	1660	–	1114	1074	1610	514	474
[Hg(H <sub>2</sub> L)Cl <sub>2</sub> ]H <sub>2</sub> O	1540	1639	1633	1679	3253	–	1081	–	500	474
[UO <sub>2</sub> (H <sub>2</sub> L)(OAc) <sub>2</sub> ]H <sub>2</sub> O	1535	1643	1620	1681	3255	–	1080	–	514	447

Chr: chromonaldehyde.

\* New azomethine band.



Structure 2.

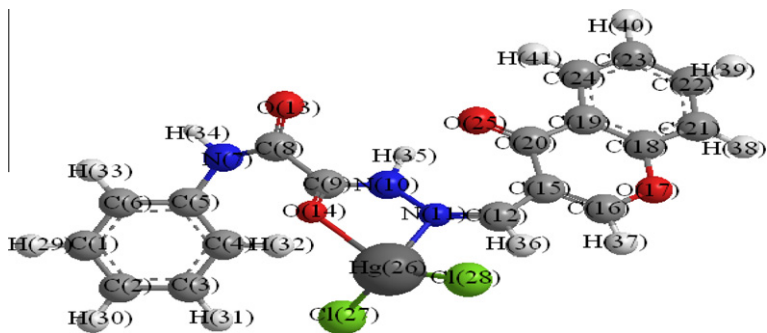
ing in the usual range as reported earlier [26] and extremely in accordance with that calculated by the use of MM + force field (as implemented in hyperchem 8.0) [12].

Also, H<sub>2</sub>L behaves as neutral ONO tridentate ligand through C=N(azomethine), C=O<sup>3</sup>(hydrazonic) and (C=O)(chromonic) groups in [Cu(H<sub>2</sub>L)Cl<sub>2</sub>(H<sub>2</sub>O)]H<sub>2</sub>O (Structure 4). This behavior is suggested by the shift of  $\nu(\text{C}=\text{O})$ (chromonic),  $\nu(\text{C}=\text{N})$ (azomethine) and  $\nu(\text{C}=\text{O})^2$ (hydrazonic) vibrations to lower wavenumber.

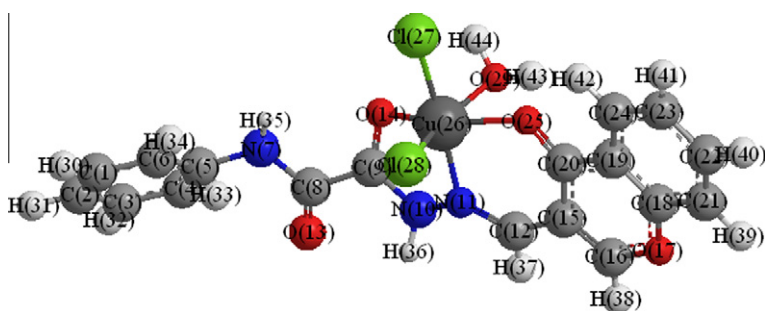
Finally, HOCAH coordinates in mononegative ONO tridentate manner in [Ni(HL)Cl] (Structure 5), [Cd(HL)Cl]H<sub>2</sub>O (Structure 6) and [Zn(HL)(OAc)]H<sub>2</sub>O (Structure 7) through C=N(azomethine), deprotonated carbonyl oxygen (=C–O<sup>–</sup>)<sup>3</sup>(hydrazonic) and

(C=O)(chromonic) groups. This mode of chelation is confirmed by the following observations; (i) A shift of  $\nu(\text{C}=\text{O})$ (chromonic) to lower wavenumber, (ii) A shift of  $\nu(\text{C}=\text{N})$ (azomethine) either to lower wavenumber in Ni(II) complex or to higher wavenumber in Cd(II) and Zn(II) complexes and (iii) the disappearance of bands due to  $\nu(\text{N}^4\text{H})$  and  $\nu(\text{C}=\text{O})^3$ (hydrazonic) vibrations with simultaneous appearance of new bands in the regions (1610–1616 cm<sup>–1</sup>) and (1108–1114 cm<sup>–1</sup>), respectively attributable to new  $\nu(\text{C}=\text{N})$  [27] and  $\nu(\text{C}-\text{O})$  vibrations [28].

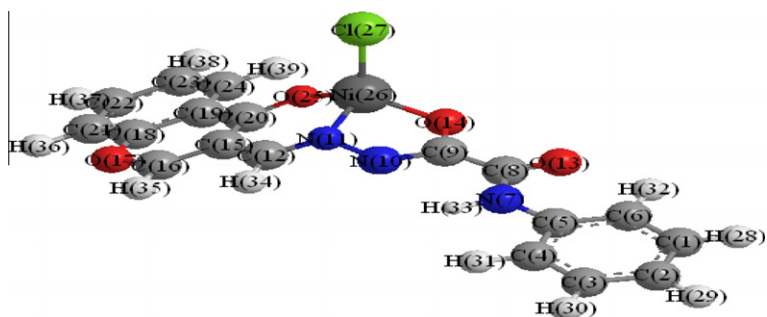
Enolization of the carbonyl oxygen (=C–O<sup>–</sup>)<sup>3</sup>(hydrazonic) is further confirmed by the absence of the signal due to N<sup>4</sup>H proton in the <sup>1</sup>H NMR spectrum of Cd(II) complex. Also, the N<sup>1</sup>H proton



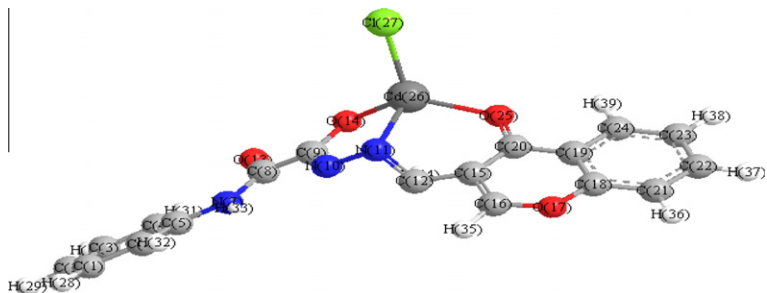
Structure 3.



Structure 4.



Structure 5.

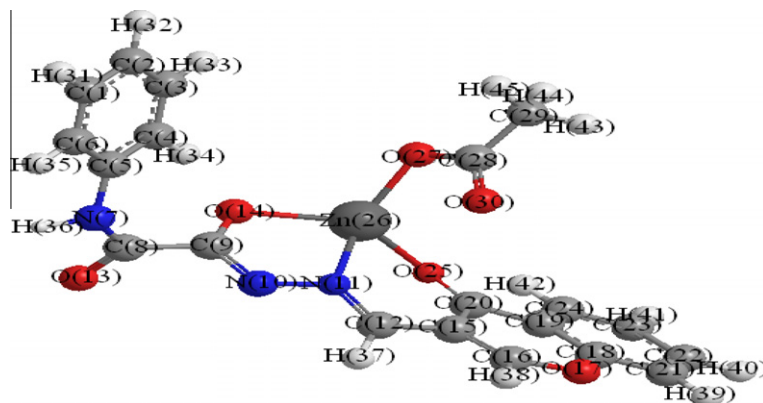


Structure 6.

appeared singlet at 10.60 ppm nearly at the same position that observed in  $H_2L$  ligand.

New bands observed in all complexes at 500–514 and 434–474  $cm^{-1}$  tentatively assigned to  $\nu(M-O)$  [29] and  $\nu(M-N)$  [30], respectively.

The broad bands at  $\approx 3399$ – $3454$ ,  $868$ – $850$ , and at  $\approx 567$   $cm^{-1}$  in the IR spectra of the investigated complexes are referred to  $\nu(OH)$ ,  $\Delta(H_2O)$ ,  $p_r(H_2O)$  and  $P_w(H_2O)$  vibrations for the coordinated water. The broad band centered at  $3500$   $cm^{-1}$  in the spectra of the studied complexes may be due to hydrated water. To verify between the



Structure 7.

**Table 3**  
Spectral absorption bands, magnetic moments and ligand field parameters of H<sub>2</sub>L metal complexes.

Compound	Band position (cm <sup>-1</sup> )	Assignment	Ligand field parameters			$\mu_{\text{eff}}$ (BM)
			$D_q$ (cm <sup>-1</sup> )	$B$ (cm <sup>-1</sup> )	$\beta$	
[Cu(H <sub>2</sub> L)Cl <sub>2</sub> (H <sub>2</sub> O)]H <sub>2</sub> O	13,440	${}^2B_{1g} \rightarrow {}^2E_g$	–	–	–	2.08
	15,200	${}^2B_{1g} \rightarrow {}^2A_{1g}$	–	–	–	
	23,148	LMCT	–	–	–	
[Ni(HL)Cl]	17,450	${}^3T_1(F) \rightarrow {}^3T_1(P)$	–	–	–	3.6
[Co(H <sub>2</sub> L)Cl <sub>2</sub> (H <sub>2</sub> O) <sub>2</sub> ]	14,880	${}^4T_{1g}(F) \rightarrow {}^4A_{2g}(F)$	762	794	0.81	5.57
	17,860	${}^4T_{1g}(F) \rightarrow {}^4T_{1g}(P)$	–	–	–	
[UO <sub>2</sub> (H <sub>2</sub> L)(OAc) <sub>2</sub> ]H <sub>2</sub> O	21,930	${}^1\Sigma_g^+ \rightarrow {}^2\pi_4$	–	–	–	0.0
	27,625	$n \rightarrow \pi^*$	–	–	–	
[Zn(HL)(OAc)]H <sub>2</sub> O	24,271	Charge transfer	–	–	–	0.0
	22,222		–	–	–	

LMCT: ligand to metal charge transfer.

**Table 4**  
Decomposition steps with the temperature range and weight loss for H<sub>2</sub>L complexes.

Complex	Temp. range (°C)	Removed species	Wt. loss	
			Found (%)	Calcd (%)
[Cu(H <sub>2</sub> L)Cl <sub>2</sub> H <sub>2</sub> O]H <sub>2</sub> O	31–112	–H <sub>2</sub> O	3.45	3.56
	113–240	–(H <sub>2</sub> O + 0.5Cl <sub>2</sub> )	10.65	10.56
	241–389	–(C <sub>6</sub> H <sub>6</sub> N + 0.5Cl <sub>2</sub> )	25.01	25.22
	390–555	–(C <sub>3</sub> N <sub>2</sub> OH)	16.17	16.02
	556–779	–C <sub>9</sub> H <sub>5</sub> O <sub>2</sub>	28.45	28.69
	780–800	–CuO(residue)	15.52	15.72
[Ni(HL)Cl]	338–480	–(C <sub>6</sub> H <sub>6</sub> N + CO + C <sub>2</sub> N <sub>2</sub> H + 0.5Cl <sub>2</sub> )	48.88	48.68
	480–589	–C <sub>9</sub> H <sub>5</sub> O <sub>2</sub>	33.11	33.87
	590–800	–NiO(residue)	17.98	17.43
[Cd(HL)Cl]H <sub>2</sub> O	34–116	–H <sub>2</sub> O	3.33	3.60
	224–422	–(C <sub>7</sub> H <sub>6</sub> NO + 0.5Cl <sub>2</sub> )	31.25	31.10
	423–589	–C <sub>2</sub> N <sub>2</sub> H	11.31	10.60
	743–795	–C <sub>9</sub> H <sub>5</sub> O <sub>2</sub>	28.50	29.01
	796–800	–CdO(residue)	25.54	25.67
[Zn(HL)(OAc)]H <sub>2</sub> O	32–124	–H <sub>2</sub> O	3.75	3.77
	353–528	–(OAc + C <sub>7</sub> H <sub>6</sub> NO + C <sub>9</sub> H <sub>5</sub> O <sub>2</sub> )	67.02	68.01
	529–759	–C <sub>2</sub> N <sub>2</sub> H	12.21	11.12
	760–800	–ZnO(residue)	16.98	17.06

coordinated and hydrated water, TGA measurement was carried out.

### 3.2. Electronic spectra and magnetic measurements

The  $n \rightarrow \pi^*$  transitions associated to the azomethine and carbonyl functions of the ligand could not be displayed because its

insolubility. Electronic spectra of metal complexes were measured in dimethylsulfoxide (DMSO) solution. The tentative assignments of the significant spectral absorption bands, magnetic moments and ligand field parameters of metal complexes are given in Table 3.

The electronic spectrum of [Cu(H<sub>2</sub>L)Cl<sub>2</sub>(H<sub>2</sub>O)]H<sub>2</sub>O shows two bands at 13,440 and 15,197 cm<sup>-1</sup> attributable to  ${}^2B_{1g} \rightarrow {}^2E_g$  and

${}^2B_{1g} \rightarrow {}^2A_{1g}$  transitions, respectively, in an octahedral geometry [29,31]. A new absorption at  $23,148\text{ cm}^{-1}$  was attributed to a ligand to metal charge transfer transition. The magnetic moment value is higher than normal range of copper (II) complexes which may be referred to spin-orbital coupling [32].

The electronic spectrum of the  $[\text{Ni}(\text{HL})\text{Cl}]$  exhibits a broad band at  $17,452\text{ cm}^{-1}$  assigned to  ${}^3T_1(\text{F}) \rightarrow {}^3T_1(\text{P})$  transition. The band position and the magnetic moment value (Table 3) can be taken as evidence for the tetrahedral stereochemistry [33].

The electronic spectrum of  $[\text{Co}(\text{H}_2\text{L})\text{Cl}_2(\text{H}_2\text{O})_2]$  shows two bands at  $14,880$  and  $17,857\text{ cm}^{-1}$  assignable to the  ${}^4T_{1g}(\text{F}) \rightarrow {}^4A_{2g}(\text{F})$  and  ${}^4T_{1g}(\text{F}) \rightarrow {}^4T_{1g}(\text{P})$  transitions, respectively, for octahedral geometry [34]. The magnetic moment value ( $\mu_{\text{eff}} = 5.57\text{ BM}$ ) and the ligand field parameters are further evidence for octahedral  $\text{Co}(\text{II})$  complexes [35]. The high value of  $\mu_{\text{eff}}$  may be due to high orbital contribution.

Finally, the spectrum of  $[\text{UO}_2(\text{H}_2\text{L})(\text{OAc})_2]\text{H}_2\text{O}$  exhibits two bands, the first one at  $27,624\text{ cm}^{-1}$  due to a charge transfer, probably  $\text{H}_2\text{L} \rightarrow \text{O}=\text{U}=\text{O}$ , while the second band at  $21,929\text{ cm}^{-1}$  may be assigned to the  ${}^1\Sigma_g^+ \rightarrow {}^2\pi_g$  transition [36].

### 3.3. Thermogravimetric studies

The stages of decomposition, temperature range, decomposition product as well as the weight loss percentages of some metal complexes are given in Table 4. Fig. 1 shows the TGA curves of some metal complexes.  $[\text{Cu}(\text{H}_2\text{L})\text{Cl}_2\text{H}_2\text{O}]\text{H}_2\text{O}$  a representative example.

In its TG thermogram, the first stage at  $31\text{--}112\text{ }^\circ\text{C}$  with weight loss of 3.45 (Calcd. 3.56%) is corresponding to the loss of one lattice water molecule. The second step with weight loss of 10.65 (Calcd. 10.56%) at  $113\text{--}240\text{ }^\circ\text{C}$  is attributed to the elimination of  $\text{H}_2\text{O} + 0.5\text{Cl}_2$ . The third step at  $241\text{--}389\text{ }^\circ\text{C}$  with weight loss of 25.01 (Calcd. 25.22%) is referring to the removal of  $\text{C}_6\text{H}_6\text{N} + 0.5\text{Cl}_2$ . The fourth step corresponds to the elimination of  $\text{C}_3\text{N}_2\text{OH}$  with weight loss of 16.17 (Calcd. 16.02%). This is followed by loss of  $\text{C}_9\text{H}_5\text{O}_2$  fragment with weight loss of 28.45 (Calcd. 28.69%). The residual part is  $\text{CuO}$  (Found 15.52, Calcd. 15.72%). An inspection of the data represented in Table 4 indicates that the TG thermograms displayed a high residual part for the studied complexes reflecting a higher thermal stability owing to the existence of five membered rings.

### 3.4. Kinetic data

The kinetic and thermodynamic parameters of the thermal degradation process have been calculated using Coats–Redfern and Horowitz–Metzger models [37,38]. Coats–Redfern relation is as follows:

$$\ln \left[ -\frac{\ln(1-\alpha)}{T^2} \right] = \ln \left( \frac{AR}{\beta E} \right) - \frac{E}{RT} \quad (1)$$

where  $\alpha$  represents the fraction of sample decomposed at time  $t$ , defined by:  $\alpha = \frac{w_0 - w_t}{w_0 - w_\infty}$ ,  $w_0$ ,  $w_t$  and  $w_\infty$  are the weight of the sample be-

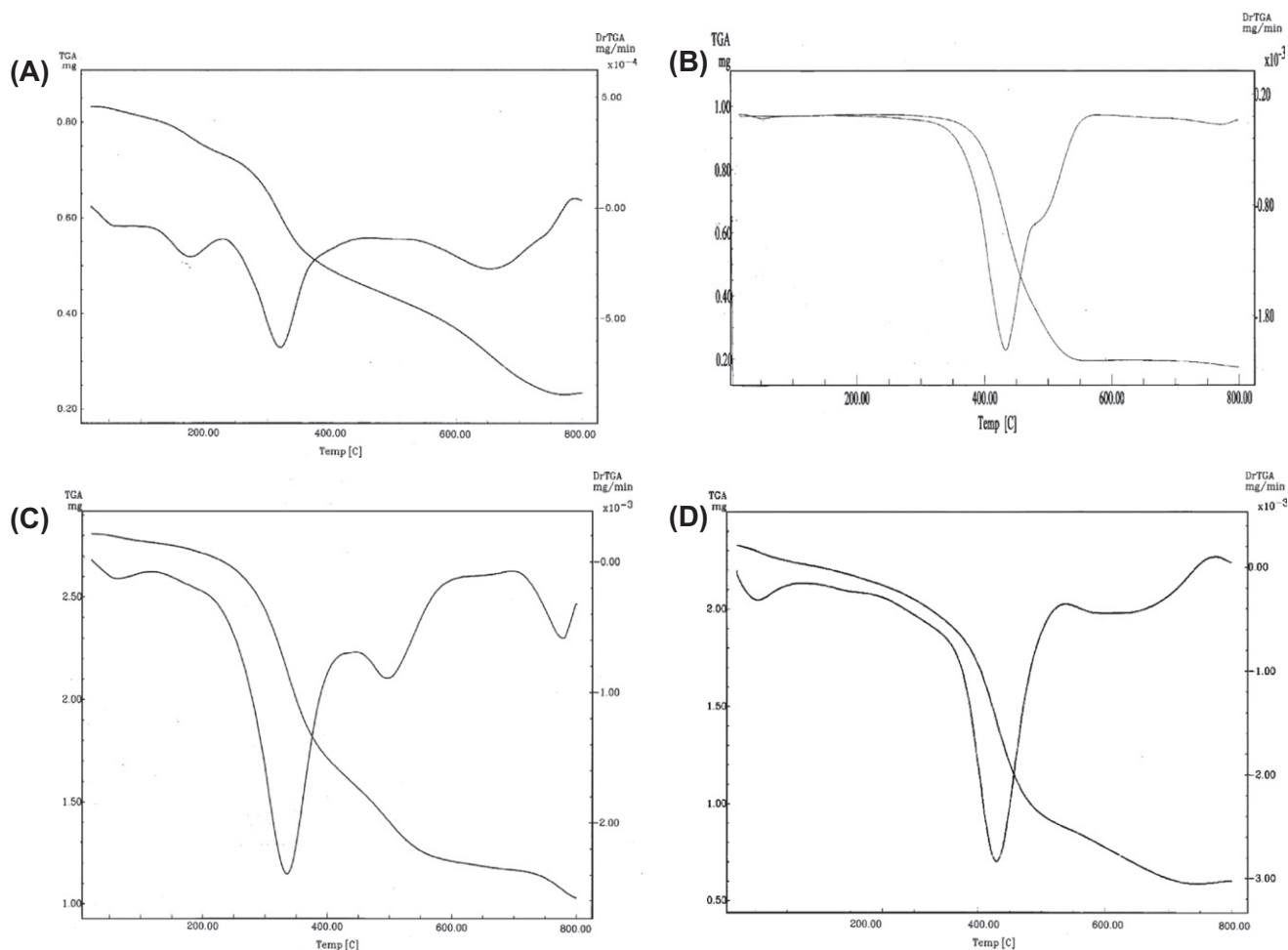


Fig. 1. (A) Thermal analysis curve (TGA, DTG) of  $[\text{Cu}(\text{H}_2\text{L})\text{Cl}_2\text{H}_2\text{O}]\text{H}_2\text{O}$ . (B) Thermal analysis curve (TGA, DTG) of  $[\text{Ni}(\text{HL})\text{Cl}]$ . (C) Thermal analysis curve (TGA, DTG) of  $[\text{Cd}(\text{HL})\text{Cl}]\text{H}_2\text{O}$ . (D) Thermal analysis curve (TGA, DTG) of  $[\text{Zn}(\text{HL})(\text{OAc})]\text{H}_2\text{O}$ .

**Table 5**Kinetic parameters evaluated by Coats–Redfern equation for H<sub>2</sub>L complexes.

Complex coats	Peak	Mid temp (K)	$E_a$ (kJ/mol)	$A$ (S <sup>-1</sup> )	$\Delta H^*$ (kJ/mol)	$\Delta S^*$ (kJ/mol K)	$\Delta G^*$ (kJ/mol)
[Ni(HL)Cl]	1st	682	161.99	$3.42 \times 10^5$	156.32	-0.145	255.87
	2nd	800	230.64	$8.61 \times 10^5$	223.99	-0.139	335.65
[Cu(H <sub>2</sub> L)Cl <sub>2</sub> (H <sub>2</sub> O) <sub>2</sub> ]H <sub>2</sub> O	1st	344	53.97	$3.57 \times 10^4$	51.11	-0.158	105.78
	2nd	449	57.67	$6.68 \times 10^4$	53.94	-0.155	123.96
	3rd	587	86.46	$7.88 \times 10^4$	81.58	-0.156	173.63
	4th	745	90.89	$1.80 \times 10^5$	84.70	-0.151	197.85
	5th	941	153.38	$2.78 \times 10^5$	145.56	-0.150	286.92
[Zn(HL)(OAc)]H <sub>2</sub> O	1st	350	54.02	$6.01 \times 10^4$	51.11	-0.154	105.27
	2nd	713	111.99	$1.36 \times 10^5$	106.06	-0.153	215.76
	3rd	918	138.31	$1.73 \times 10^5$	130.68	-0.153	272.00
[Cd(HL)Cl]H <sub>2</sub> O	1st	348	45.44	$3.00 \times 10^4$	42.55	-0.160	98.39
	2nd	596	74.21	$1.20 \times 10^5$	69.25	-0.153	160.67
	3rd	779	108.25	$3.55 \times 10^5$	101.78	-0.146	216.01
	4th	1042	690.94	$3.38 \times 10^6$	682.28	-0.130	818.08

fore the degradation, at temperature  $t$  and after total conversion, respectively.  $T$  is the derivative peak temperature.  $\beta$  is the heating rate =  $dT/dt$ ,  $E$  and  $A$  are the activation energy and the Arrhenius pre-exponential factor, respectively. A plot of  $\ln[-\frac{\ln(1-\alpha)}{T^2}]$  versus  $1/T$  gives a straight line whose slope ( $E/R$ ) and the pre-exponential factor ( $A$ ) can be determined from the intercept.

The Horowitz–Metzger relation [38] used to evaluate the degradation kinetics is:

$$\ln[-\ln(1-\alpha)] = \frac{E\theta}{RT_s^2} \quad (2)$$

where  $\theta = T - T_s$ ,  $T_s$  is the DTG peak temperature,  $T$  is the temperature corresponding to weight loss  $W_t$ . A straight line should be observed between  $\ln[-\ln(1-\alpha)]$  and  $\theta$  with a slope of  $\frac{E}{RT_s^2}$ . A number of degradation processes can be represented as a first order reaction. Particularly, the degradation of a series of H<sub>2</sub>L complexes was suggested to be first order [39], therefore we assume  $n = 1$  for the remainder. The other thermodynamic parameters of activation can be calculated by Eyring equation [40]:

$$\Delta H^* = E - RT \quad (3)$$

$$\Delta S^* = R \ln \frac{hA}{k_B T} \quad (4)$$

$$\Delta G^* = \Delta H - T\Delta S \quad (5)$$

Thermodynamic parameters such as activation energy ( $E$ ), pre-exponential factor ( $A$ ), entropy of activation ( $\Delta S$ ), enthalpy of activation ( $\Delta H$ ) and free energy of activation ( $\Delta G$ ) of decomposition steps were calculated using Coats–Redfern [37] and Horowitz–

Metzger [38] methods (Tables 5 and 6). In both methods, the lift side of Eqs. (3) and (4) are plotted against  $1/T$  and  $\theta$ , respectively (Figs. 2–9). From the results, the following remarks can be pointed out:

- The high values of the energy of activation,  $E$  of the complexes reveals the high stability of such chelates due to their covalent bond character [41].
- The positive sign of  $\Delta G$  for the investigated complexes reveals that the free energy of the final residue is higher than that of the initial compound, and all the decomposition steps are non-spontaneous processes. Also, the values of the activation,  $\Delta G$  increases significantly for the subsequent decomposition stages of a given complex. This is due to increasing the values of  $T\Delta S$  significantly from one step to another which overrides the values of  $\Delta H$  [42–44].
- The negative values of  $\Delta S$  for the degradation process indicates more ordered activated complex than the reactants or the reaction is slow [40].

### 3.5. Molecular modeling

The molecular structure along with atom numbering of H<sub>2</sub>L and its metal complexes are shown in Structures 1–7. Analysis of the data in Tables 1S–14S (Supplementary materials) calculated for the bond lengths and angles for the bond, one can conclude the following remarks:

**Table 6**Kinetic parameters evaluated by Horowitz–Metzger equation for H<sub>2</sub>L complexes.

Complex Horowitz	Peak	Mid temp (K)	$E_a$ (kJ/mol)	$A$ (S <sup>-1</sup> )	$\Delta H^*$ (kJ/mol)	$\Delta S^*$ (kJ/mol K)	$\Delta G^*$ (kJ/mol)
[Ni(HL)Cl]	1st	682	161.70	$3.56 \times 10^5$	156.02	-0.145	255.34
	2nd	808	230.81	$8.70 \times 10^5$	224.09	-0.139	336.84
[Cu(H <sub>2</sub> L)Cl <sub>2</sub> (H <sub>2</sub> O) <sub>2</sub> ]H <sub>2</sub> O	1st	344	53.79	$3.69 \times 10^4$	50.93	-0.158	105.51
	2nd	449	57.57	$7.41 \times 10^4$	53.84	-0.155	123.47
	3rd	587	86.05	$7.62 \times 10^4$	81.17	-0.157	173.38
	4th	745	90.72	$1.85 \times 10^5$	84.52	-0.151	197.51
	5th	941	153.86	$2.85 \times 10^5$	146.04	-0.150	287.21
[Zn(HL)(OAc)]H <sub>2</sub> O	1st	350	54.99	$6.58 \times 10^4$	52.08	-0.154	105.98
	2nd	713	111.37	$1.35 \times 10^5$	105.44	-0.153	215.19
	3rd	918	138.72	$1.74 \times 10^5$	131.09	-0.153	272.40
[Cd(HL)Cl]H <sub>2</sub> O	1st	348	45.75	$3.08 \times 10^4$	42.85	-0.160	98.63
	2nd	596	74.51	$1.22 \times 10^5$	69.55	-0.153	160.88
	3rd	779	108.01	$3.80 \times 10^5$	101.54	-0.146	215.33
	4th	1042	690.65	$3.16 \times 10^6$	681.99	-0.130	818.37

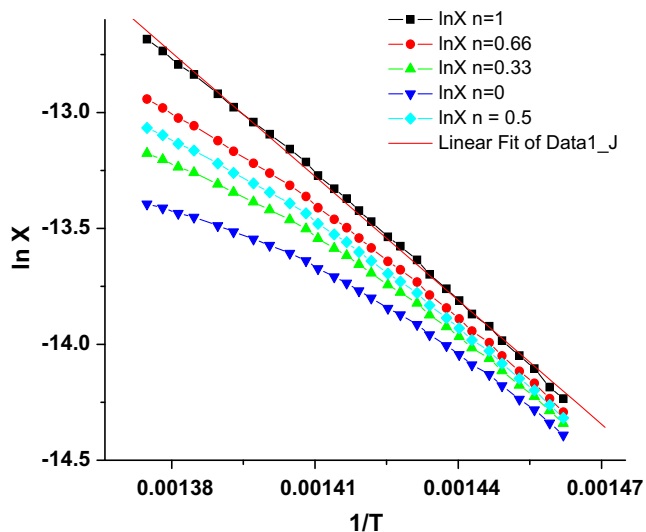


Fig. 2. Coats–Redfern plots first degradation steps for [Ni(HL)Cl] complex.

1. The N(10)–N(11) and N(11)–C(14) bond lengths becomes slightly longer in complexes as the coordination takes place via N atoms of  $-C=N-N=C-$  group that is formed on deprotonation of OH group in [Ni(HL)Cl], [Cd(HL)Cl]H<sub>2</sub>O and [Zn(HL)(OAc)]H<sub>2</sub>O complexes [14].
2. In [Ni(HL)Cl], [Cd(HL)Cl]H<sub>2</sub>O and [Zn(HL)(OAc)]H<sub>2</sub>O complexes, C(9)–O(13) and C(9)–N(10) bond distances are elongated and shortened, respectively. This is referred to the formation of the M–O bond which makes the C–O bond weaker and forming a double bond character [45]. On the other hand, in [Co(H<sub>2</sub>L)Cl<sub>2</sub>(H<sub>2</sub>O)<sub>2</sub>] and [Hg(H<sub>2</sub>L)Cl<sub>2</sub>]H<sub>2</sub>O complexes, this bond distance remains practically unaltered indicating that this group is not participated in bonding [46].
3. The bond angles of the hydrazone moiety of H<sub>2</sub>L are altered somewhat upon coordination but the angles around the metal undergo appreciable variations upon changing the metal center [46]; the largest change affects C(9)–N(10)–N(11),

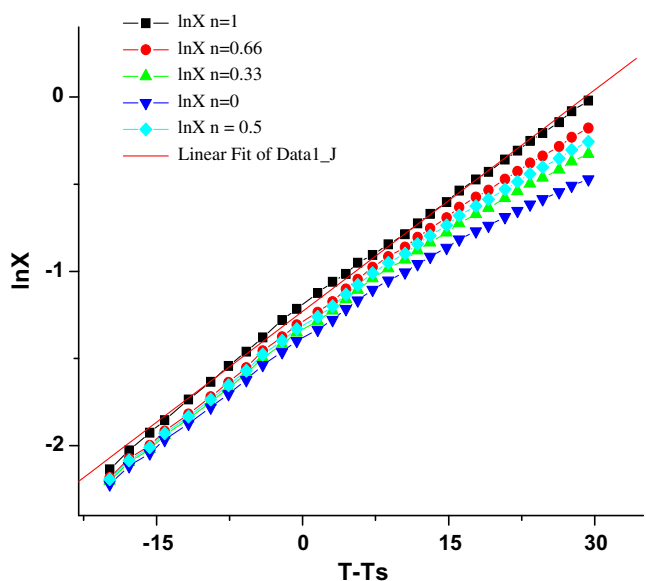


Fig. 3. Horowitz–Metzger plot of first degradation step for [Ni(HL)Cl] complex.

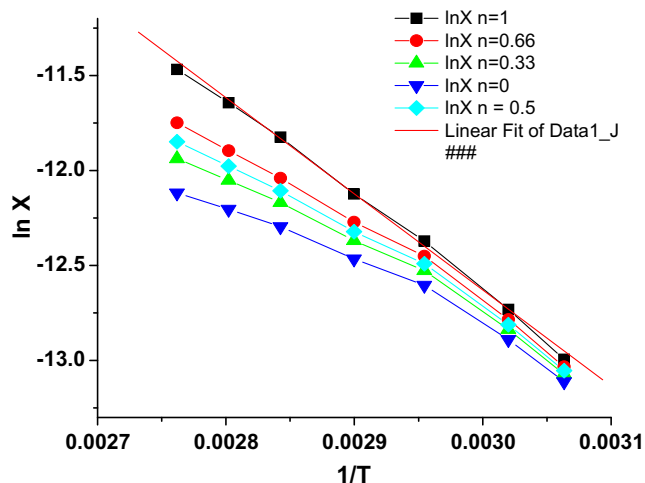


Fig. 4. Coats–Redfern plot of first degradation step for [Cu(H<sub>2</sub>L)Cl<sub>2</sub>(H<sub>2</sub>O)]H<sub>2</sub>O complex.

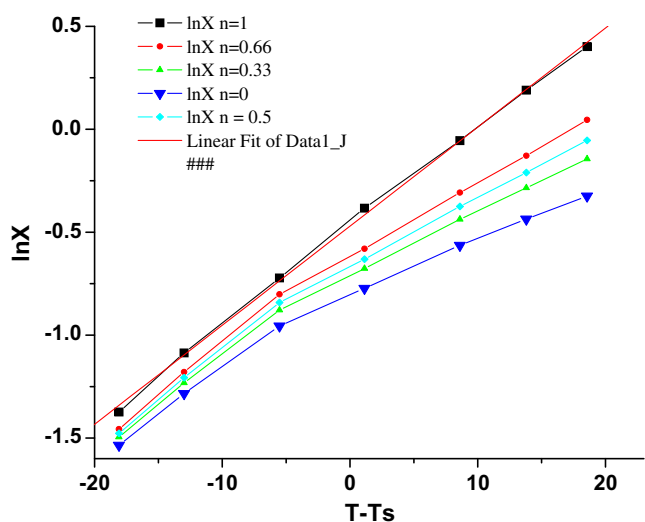


Fig. 5. Horowitz–Metzger plot of first degradation step for [Cu(H<sub>2</sub>L)Cl<sub>2</sub>(H<sub>2</sub>O)]H<sub>2</sub>O complex.

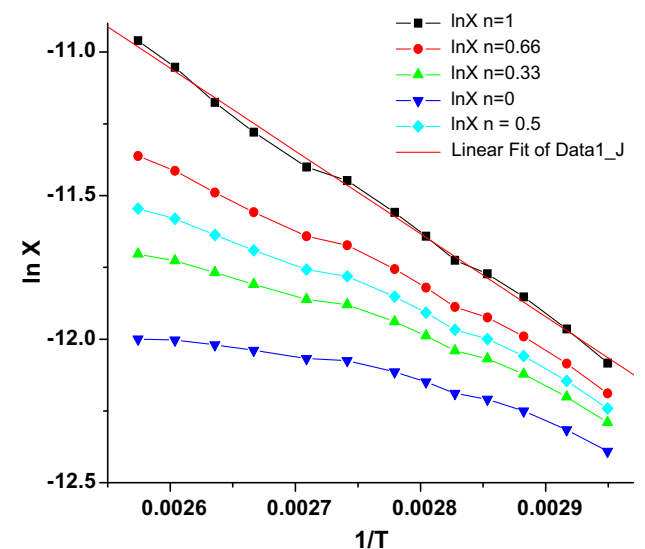


Fig. 6. Coats–Redfern plot of first degradation step for [Zn(HL)(OAc)]H<sub>2</sub>O complex.

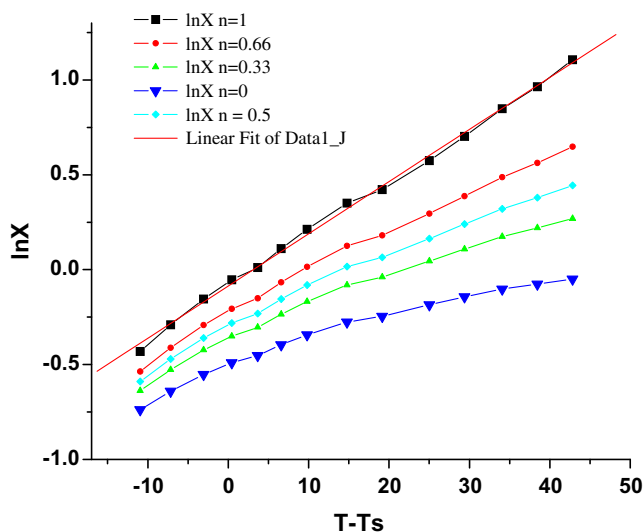


Fig. 7. Horowitz–Metzger plot of first degradation step for  $[\text{Zn}(\text{HL})(\text{OAc})]\text{H}_2\text{O}$  complex.

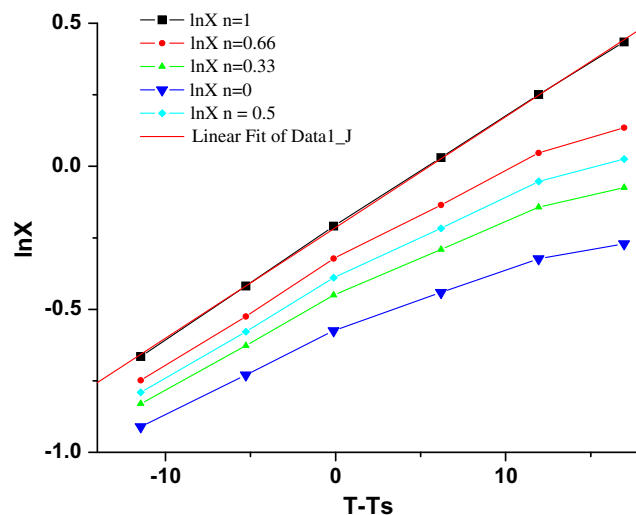


Fig. 9. Horowitz–Metzger plot of first degradation step for  $[\text{Cd}(\text{HL})\text{Cl}]\text{H}_2\text{O}$  complex.

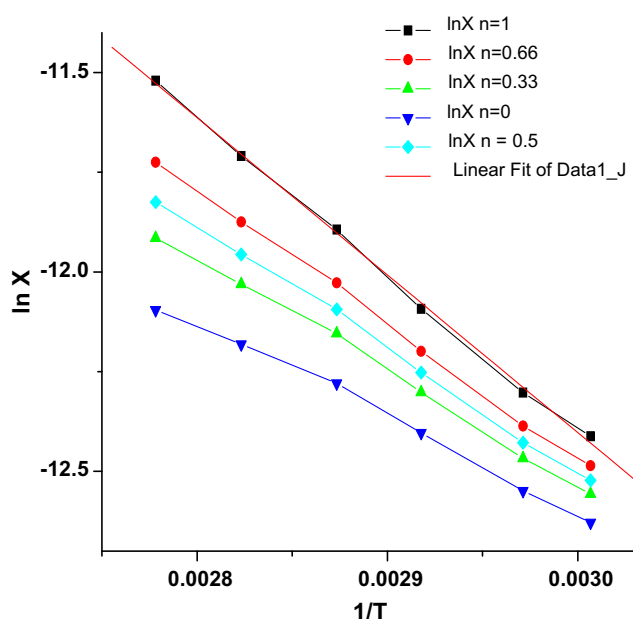


Fig. 8. Coats–Redfern plot of first degradation step for  $[\text{Cd}(\text{HL})\text{Cl}]\text{H}_2\text{O}$  complex.

$\text{O}(13)\text{—C}(9)\text{—N}(10)$  and  $\text{O}(13)\text{—C}(9)\text{—C}(8)$  angles which are reduced or increased on complex formation as a consequence of bonding [14].

Table 7  
Some energetic properties of  $\text{H}_2\text{L}$  and its complexes calculated by PM3 method.

Compound	Total energy (kcal/mol)	Binding energy (kcal/mol)	Electronic energy (kcal/mol)	Heat of formation (kcal/mol)	Dipole moment (D)	HOMO (eV)	LUMO (eV)
$\text{H}_2\text{L}$	$-9.20 \times 10^4$	-4363.36	$-6.21 \times 10^5$	-32.78	2.04	-9.20	-0.80
$[\text{Cu}(\text{H}_2\text{L})\text{Cl}_2(\text{H}_2\text{O})]\text{H}_2\text{O}$	$-1.41 \times 10^5$	-4784.26	$-1.01 \times 10^6$	-151.23	5.87	-4.20	-1.26
$[\text{Co}(\text{H}_2\text{L})\text{Cl}_2(\text{H}_2\text{O})_2]$	$-1.40 \times 10^5$	-5294.86	$-1.06 \times 10^6$	-476.38	2.99	-4.03	-1.39
$[\text{Hg}(\text{H}_2\text{L})\text{Cl}_2]\text{H}_2\text{O}$	$-1.07 \times 10^5$	-4505.53	$-7.94 \times 10^5$	-102.28	11.45	-9.38	-1.90
$[\text{Ni}(\text{HL})\text{Cl}]$	$1.23 \times 10^5$	-4621.17	$-8.17 \times 10^5$	-210.90	12.47	-7.88	-1.94
$[\text{Cd}(\text{HL})\text{Cl}]\text{H}_2\text{O}$	$-9.95 \times 10^4$	-4353.57	$-6.85 \times 10^5$	-19.38	4.72	-8.94	-0.98
$[\text{Zn}(\text{HL})(\text{OAc})]\text{H}_2\text{O}$	$-1.12 \times 10^5$	-4991.80	$-8.40 \times 10^5$	-64.94	8.39	-8.64	-1.67

4. The lower HOMO energy values show that molecules donating electron ability is the weaker. On contrary, the higher HOMO energy implies that the molecule is a good electron donor. LUMO energy represents the ability of a molecule receiving electron as in Table 7 [47].

### 3.6. Antimicrobial activity

The biological activity of  $\text{H}_2\text{L}$  and its complexes against *B. thuringiensis* (*Bt*) as Gram positive bacteria and *P. aeruginosa* (*Pa*) as Gram negative bacteria is summarized in Table 8. It is clear that the complexes exhibit high inhibition activity against bacteria *Bt* and *Pa*.

$[\text{Cd}(\text{HL})\text{Cl}]\text{H}_2\text{O}$  and  $[\text{UO}_2(\text{H}_2\text{L})(\text{OAc})_2]\text{H}_2\text{O}$  complexes exhibited high inhibitory effects on *Bt* while  $[\text{Hg}(\text{H}_2\text{L})\text{Cl}_2]\text{H}_2\text{O}$  complex against *Pa* organisms. The lowest one is  $\text{H}_2\text{L}$ . This can be attributed to the ability of the complexes to diffuse into the cell membrane of the organism. Examining the values for Gram's positive bacteria in Table 5, one can arrange the compounds as:  $[\text{Cd}(\text{HL})\text{Cl}]\text{H}_2\text{O} > [\text{UO}_2(\text{H}_2\text{L})(\text{OAc})_2]\text{H}_2\text{O} > [\text{Hg}(\text{H}_2\text{L})\text{Cl}_2]\text{H}_2\text{O} > [\text{Co}(\text{H}_2\text{L})\text{Cl}_2(\text{H}_2\text{O})_2] > [\text{Ni}(\text{HL})\text{Cl}] > [\text{Zn}(\text{HL})(\text{OAc})]\text{H}_2\text{O} > [\text{Cu}(\text{H}_2\text{L})\text{Cl}_2(\text{H}_2\text{O})]\text{H}_2\text{O} > \text{H}_2\text{L}$ .

On the other hand, the inhibition activity values against Gram's negative can arrange the compounds as:  $[\text{Hg}(\text{H}_2\text{L})\text{Cl}_2]\text{H}_2\text{O} > [\text{Cd}(\text{HL})\text{Cl}]\text{H}_2\text{O} > [\text{Ni}(\text{HL})\text{Cl}] > [\text{UO}_2(\text{H}_2\text{L})(\text{OAc})_2]\text{H}_2\text{O} > [\text{Zn}(\text{HL})(\text{OAc})]\text{H}_2\text{O} > [\text{Co}(\text{H}_2\text{L})\text{Cl}_2(\text{H}_2\text{O})_2]$ .

## 4. Conclusion

The complexes:  $[\text{UO}_2(\text{H}_2\text{L})(\text{OAc})_2]\text{H}_2\text{O}$ ,  $[\text{Co}(\text{H}_2\text{L})\text{Cl}_2(\text{H}_2\text{O})_2]$ ,  $[\text{Ni}(\text{HL})\text{Cl}]$ ,  $[\text{Cd}(\text{HL})\text{Cl}]\text{H}_2\text{O}$ ,  $[\text{Zn}(\text{HL})(\text{OAc})]\text{H}_2\text{O}$ ,  $[\text{Hg}(\text{H}_2\text{L})\text{Cl}_2]\text{H}_2\text{O}$ ,  $[\text{Cu}(\text{H}_2\text{L})\text{Cl}_2(\text{H}_2\text{O})]\text{H}_2\text{O}$  have been synthesized with 2-oxo-N'-(4-

**Table 8**Antibacterial activities in terms of inhibition zone diameter (mm) of H<sub>2</sub>L and its metal complexes.

Compound	Zone of inhibition of bacterial growth (mm)	
	<i>Bacillus thuringiensis</i> (Gram-positive)	<i>Pseudomonas aeruginosa</i> (Gram-negative)
Gentamicin	48	48
H <sub>2</sub> L	35	0
[Cu(H <sub>2</sub> L)Cl <sub>2</sub> (H <sub>2</sub> O)]H <sub>2</sub> O	40	0
[Co(H <sub>2</sub> L)Cl <sub>2</sub> (H <sub>2</sub> O) <sub>2</sub> ]	56	14
[Ni(HL)Cl]	54	44
[Cd(HL)Cl]H <sub>2</sub> O	71	47
[Zn(HL)(OAc)]H <sub>2</sub> O	48	26
[Hg(H <sub>2</sub> L)Cl <sub>2</sub> ]H <sub>2</sub> O	65	48
[UO <sub>2</sub> (H <sub>2</sub> L)(OAc) <sub>2</sub> ]H <sub>2</sub> O	71	30

oxo-4H-chromen-3-yl)methylene)-2-(phenylamino)acetohydrazide (H<sub>2</sub>L). Different structures have been proposed: octahedral geometry for Co(II), Cu(II) and U(VI)O<sub>2</sub><sup>2+</sup>, a tetrahedral structure for Ni(II), Cd(II), Zn(II) and Hg(II). Cd(II) and U(VI)O<sub>2</sub><sup>2+</sup> complexes exhibited high inhibitory effects on *B. thuringiensis* (Bt) while Hg(II) complex against *P. aeruginosa* (Pa) organisms.

### Appendix A. Supplementary material

Supplementary data associated with this article can be found, in the online version, at doi:10.1016/j.molstruc.2011.03.043.

### References

- [1] S. Rollas, S.G. Küçükgül, *Molecules* 12 (2007) 1910.
- [2] P. Vicini, M. Incerti, I.A. Doytchinova, P. La Colla, B. Busonera, R. Loddio, *Eur. J. Med. Chem.* 41 (2006) 624.
- [3] H.J.C. Bezerra-Netto, D.I. Lacerda, A.L.P. Miranda, H.M. Alves, E.J. Barreiro, C.A.M. Fraga, *Bioorg. Med. Chem.* 14 (2006) 7924.
- [4] Y.P. Kitaev, B.I. Buzykin, T.V. Troepolskaya, *Russ. Chem.* 4 (2006) 624.
- [5] O. Pouralimardan, A.C. Chamayou, C. Janiak, H. Hosseini-Monfared, *Inorg. Chim. Acta* 360 (2007) 1599.
- [6] C. Basu, S. Chowdhury, R. Banerjee, H.S. Evans, S. Mukherjee, *Polyhedron* 26 (2007) 3617.
- [7] M. Bakir, O. Green, W.H. Mulder, *J. Mol. Struct.* 873 (2008) 17.
- [8] J.L. Buss, J. Neuzil, P. Ponka, *Biochem. Soc. Trans.* 30 (2002) 755.
- [9] P. Foltinová, M. Lácová, D. Loos, *Il Farmaco*. 55 (2000) 21.
- [10] N.N. Das, A.C. Dash, *Polyhedron* 15 (1996) 1751.
- [11] R.P. John, A. Srekanth, V. Rajakannan, T.A. Ajith, M.R.P. Kurup, *Polyhedron* 23 (2004) 2549.
- [12] HyperChem version 8.0 Hypercube, Inc.
- [13] N.L. Alpert, W.E. Keiser, H. Szmanski, *A Theory and Practice of Infrared Spectroscopy*, Plenum Press, New York, 1995.
- [14] O.A. El-Gammal, *Spectrochim. Acta* 75 (A) (2010) 533.
- [15] P.B. Sreeja, M.R.P. Kurup, A. Kishore, C. Jasmin, *Polyhedron* 23 (2004) 575.
- [16] U. El-Ayaan, I.M. Kenawy, Y.G. Abu El-Reash, *J. Mol. Struct.* 871 (2007) 14.
- [17] U. El-Ayaan, G.A. EL-Reash, I.M. Kenawy, *Synth. React. Inorg. Met. – Org. Chem.* 33 (2003) 329.
- [18] J. Chakraborty, G. Pilet, M.S. El. Fallah, J. Ribas, S. Mitra, *Polyhedron* 10 (2007) 489.
- [19] H.M. El-Shaer, P. Foltinova, M. Lacova, J. Chovancova, H. Stankovicova, *Il. Farmaco*. 53 (1998) 224.
- [20] M.V. Angelusiu, S.F. Barbuceanu, C. Draghici, G.L. Almajan, *Eur. J. Med. Chem.* 45 (2010) 2055.
- [21] K. Nakamoto, *Infrared and Raman Spectra of Inorganic and Coordination Compounds*, Wiley, New York, 1986. p. 231.
- [22] K. Chanda, P.K. Sharma, B.S. Gray, R.P. Singh, *J. Inorg. Nucl. Chem.* 42 (1980) 187.
- [23] F. Quilés, *Vib. Spectrosc.* 18 (1998) 61.
- [24] C.J. Chisholm-Brause, J.M. Berg, R.A. Matzner, D.E. Morris, *J. Colloid Interf. Sci.* 233 (2001) 38.
- [25] N. Henry, M. Lagrenée, T. Loiseau, N. Clavier, N. Dacheux, F. Abraham, *Inorg. Chem. Commun.* 14 (2011) 429.
- [26] T.H. Rakha, N. Nawar, G.M. Abu Reash, *Synth. React. Inorg. Met. – Org. Chem.* 26 (1996) 1705.
- [27] J. Chakraborty, S. Thakurta, G. Pilet, D. Luneau, S. Mitra, *Polyhedron* 28 (2009) 819.
- [28] M.E. Khalifa, M.A. Akl, S.E. Ghazy, *Chem. Pharm. Bull.* 49 (2001) 664.
- [29] B. Schrader, *Vibrational Spectroscopy of Different Classes and States of Compounds*, Weinheim, Germany, 2007.
- [30] M. Atmeh, N.R. Russell, T.E. Keyes, *Polyhedron* 27 (2008) 1690.
- [31] L. Sacconi, M. Cinmpolinic, *J. Chem. Soc.* 85 (1963).
- [32] A.A.A. Emaraa, B.A. El-Sayed, E.A.E. Ahmed, *Spectrochim. Acta* 69 (A) (2008) 757.
- [33] J.C. Bailar, H.J. Emeleus, R. Nyholm, A.F. Trotman-Dickenson, *Comprehensive Inorganic Chemistry*, vol. 3, Pergamon Press, New York, 1975.
- [34] E.I. Solomon, A.B.P. Lever, *Inorganic Electronic Structure and Spectroscopy*, Elsevier, New York, 2006.
- [35] J. Lewis, R.G. Wilms, *Modern Coordination Chemistry*, Interscience, New York, 1960.
- [36] U. El-Ayaan, M.M. Youssef, S. Al-Shihry, *J. Mol. Struct.* 936 (2009) 213.
- [37] A.W. Coats, J.P. Redfern, *Nature* 20 (1964) 68.
- [38] H.H. Horowitz, G. Metzger, *Anal. Chem.* 35 (1963) 1464.
- [39] A. Broido, *J. Polym. Sci. A* 2 (7) (1969) 1761.
- [40] A.A. Frost, R.G. Pearson, *Kinetics and Mechanisms*, Wiley, New-York, 1961.
- [41] T. Taakeyama, F.X. Quinn, *Thermal Analysis Fundamentals and Applications to Polymer Science*, John Wiley and Sons, Chichester, 1994.
- [42] P.B. Maravalli, T.R. Goudar, *Thermochim. Acta* 325 (1999) 35.
- [43] K.K.M. Yusuff, R. Sreekala, *Thermochim. Acta* 159 (1990) 357.
- [44] S.S. Kandil, G.B. El-Hefnawy, E.A. Baker, *Thermochim. Acta* 414 (2004) 105.
- [45] A.A.R. Despaigne, J.G. da Silva, A.C.M. do Carmo, O.E. Piro, E.E. Castellano, H. Beraldo, *J. Mol. Struct.* 920 (2009) 97.
- [46] A.A.R. Despaigne, J.G. da Silva, A.C.M. do Carmo, F. Sives, O.E. Piro, E.E. Castellano, H. Beraldo, *Polyhedron* 28 (2009) 3797.
- [47] S. Sagdinc, B. Koksoy, F. Kandemirli, S.H. Bayari, *J. Mol. Struct.* 917 (2009) 63.